Quantum Electronics **41** (9) 794 – 800 (2011)

NONLINEAR OPTICAL PHENOMENA

PACS numbers: 42.65.Yj; 42.65.Lm; 42.81.Dp; 42.25.Ja
DOI: 10.1070/QE2011v041n09ABEH014577

Continuous-wave parametric oscillation in polarisation-maintaining optical fibre

E.A. Zlobina, S.I. Kablukov, S.A. Babin

***Abstract*. Continuous-wave parametric oscillation in a polarisation-maintaining optical fibre has been achieved for the first time using polarisation phase matching. Up-conversion with a frequency shift of ~ 8.6 THz has been demonstrated experimentally. The single-pass optical power generated at 1017 nm in a 85-m-long Nufern PM980-XP fibre exceeded 40 mW. The conversion efficiency was 3.3 %, which is an order of magnitude higher than that reported previously for cw parametric up-conversion in the 1-μm spectral region. We compare theoretical predictions with experimental data and analyse factors that may influence output power saturation with increasing signal and pump powers.**

Keywords: *fibre optics, four-wave mixing, nonlinear frequency conversion.*

1. Introduction

Optical fibres are currently widely used for nonlinear frequency conversion of coherent radiation. In connection with this, the development and characterisation of fibre optical parametric oscillators (FOPOs) has attracted increased attention. Such light sources offer relatively high conversion efficiency and enable large frequency shifts (up to 130 THz) in the visible and near-IR spectral regions [1, 2]. FOPOs take advantage of four-wave mixing (FWM): nonlinear parametric interaction between two pump photons of frequencies ω_{p1} and ω_{p2} produces two new waves, one of which is shifted to lower frequencies (Stokes component, ω_s), and the other to higher frequencies (anti-Stokes component, ω_a). In practice, pump frequency degenerate FWM, with $\omega_{p1} = \omega_{p2}$, is often examined.

For efficient FWM, a phase matching condition should be met, which minimises the wave vector mismatch between the waves involved. In most early experiments, phase matching was achieved using the difference in phase velocity between transverse modes in multimode fibres [3, 4]. With the advent and wide use of single-mode fibres in optical systems, three new phase matching methods were proposed: operation near the zero-dispersion wavelength of the fibre, operation in the anomalous group velocity dispersion region and the use of birefringent (polarisation-maintaining) fibres.

The advent of erbium-doped fibre lasers and amplifiers and highly nonlinear dispersion-shifted fibres enabled the development of FOPOs [5 – 10] around 1.55 μm, where pure silica has a transmission window. In this range, cw pumping led to the generation of a Stokes wave of power up to 38 mW [6] (linear cavity configuration for the anti-Stokes component) or even 1 W [10] (ring cavity for the anti-Stokes component). The anti-Stokes power was, however, much lower: within 100 mW in Ref. [10].

Ytterbium fibre lasers, which operate in the range 1.03 – 1.13 μm, offer high output power density, which makes them attractive optical sources for studies of nonlinear processes in optical fibres. Phase matching near 1 μm is however only possible in special photonic crystal fibres, so there has been little work in this area of research [11, 12]. On the other hand, the phase matching condition can be met in birefringent fibres. To this end, pulsed solid-state lasers were used as 1-μm pump sources in early studies [13 – 15].

In birefringent fibres, phase matching can be achieved through compensation for the material dispersion due to the difference in phase velocity between waves propagating in different polarisation modes of the fibre. As shown by Jain and Stenersen [16], the phase matching condition can be met in five ways, depending on the polarisation of the four waves. In practice, however, only two of them can be realised in the normal dispersion regime because of the third-order nonlinear susceptibility tensor symmetricity in isotropic media (including silica glass) [17].

In one of them, pump light is polarised along the two major axes of the fibre, and the Stokes and anti-Stokes waves resulting from FWM are polarised along the slow and fast axes, respectively. The frequency detuning is varied from 3 THz at visible pump wavelengths [18 – 20] to 6 – 9 THz near 1 μm [13, 14].

In the other approach, pump light is polarised along the slow axis of a birefringent fibre, and the Stokes and anti-Stokes components, along the fast axis. In this configuration, the frequency shift reaches 30 THz in the visible range [21] and 78 THz near 1 μm [15]. Since the frequency shift depends on the birefringence of the fibre, it can be

E.A. Zlobina, S.I. Kablukov, S.A. Babin Institute of Automation and Electrometry, Siberian Branch, Russian Academy of Sciences, prosp. Akad. Koptyuga 1, 630090 Novosibirsk, Russia;
e-mail: ZlobinaKaterina@rambler.ru, kab@iae.nsk.su, babin@iae.nsk.su

Received 29 April 2011; revision received 6 June 2011
Kvantovaya Elektronika **41** (9) 794 – 800 (2011)
Translated by O.M. Tsarev

controlled by varying the birefringence induced by heating [22], bending [23, 24] or tensile stress [25]. The use of birefringent photonic crystal fibres with suitable dispersion parameters [26] enabled the frequency shift to be increased to 64 THz at a pump wavelength of 647 nm.

In all the studies mentioned above, pulsed pumping was used, which ensured high peak powers, so parametric conversion was relatively easy to observe even in short fibres.

Here we report the first experimental demonstration of frequency conversion in a cw-pumped birefringent optical fibre. Using an unpolarised ytterbium fibre laser ($\lambda_p =$ 1048 nm) with an output power, P_p, of up to 4 W as a pump source and radiation with $\lambda_s = 1080.3$ nm as a signal seed, we obtained cw parametric oscillation with an anti-Stokes frequency shift of 8.6 THz. The optical power generated in a 85-m-long Nufern PM980-XP polarisation-maintaining fibre exceeded 40 mW. Conversion efficiency, evaluated as the ratio of the idler power at the fibre output to the input signal power [12], was 3.3 % at a 4-W pump power. At the same time, previous studies concerned with cw parametric up-conversion at wavelengths within 1 μm employed photonic crystal fibres, in which phase matching was ensured near the zero-dispersion wavelength of the fibre and the conversion efficiency did not exceed 0.3 % [12, 27, 28].

2. Theory

In degenerate FWM, the pump wave field acts on the medium through the third-order nonlinear susceptibility, $\chi^{(3)}$, producing two new waves, anti-Stokes (ω_a) and Stokes (ω_s), whose frequencies are shifted relative to the pump frequency, ω_p, and meet the conservation-of-energy principle: $\omega_p + \omega_p = \omega_a + \omega_s$. In the degenerate process, the frequency shifts are $\omega_p - \omega_s = \omega_a - \omega_p = \Omega$.

For efficient FWM, the law of conservation of momentum should be fulfilled, which reduces to the phase matching condition: the wave vector mismatch between the waves involved should be minimal, that is, $\Delta k = k_{p1} + k_{p2} - k_a - k_s = c^{-1}(n_{p1}\omega_p + n_{p2}\omega_p - n_a\omega_a - n_s\omega_s) = 0$, where c is the speed of light in vacuum, and k_j and n_j are the wave vectors and refractive indices at the pump, anti-Stokes and Stokes frequencies, respectively ($j =$ p1, p2, a, s).

The total wave vector mismatch, Δk, in an optical fibre comprises linear (Δk_L) and nonlinear (Δk_{NL}) mismatches: $\Delta k = \Delta k_L + \Delta k_{NL}$. The linear mismatch is determined by the material and waveguide dispersions of the fibre: $\Delta k_L = \Delta k_M + \Delta k_W$ [29]. The nonlinear mismatch arises from nonlinear effects in the optical fibre: self-phase modulation (SPM) and cross-phase modulation (XPM). In the case of nondegenerate pumping, Δk_{NL} depends on the nonlinearity coefficient of the fibre, γ, and the powers of the two pump waves P_1 and P_2: $\Delta k_{NL} = \gamma(P_1 + P_2)$ [29].

In the normal dispersion regime, at small frequency shifts (Ω) and a pump wavelength not too close to the zero-dispersion wavelength of the fibre, the contribution of the material dispersion can be approximately represented as $\Delta k_M = \beta_2\Omega^2$, where β_2 is the group velocity dispersion coefficient. The nonlinear term Δk_{NL} is positive, so, for the phase matching condition to be met, the waveguide dispersion contribution, Δk_W, should be made negative. As mentioned above, in birefringent fibres this can be achieved when four waves propagate with different phase velocities in two polarisation modes of the fibre. Figure 1 schematically illustrates two wave vector matching processes. The fibre is pumped in different polarisation modes in one case (Fig. 1a) and along the slow axis in the other (Fig. 1b). The frequency shift of the sidebands relative to the pump frequency is markedly larger in the latter case.

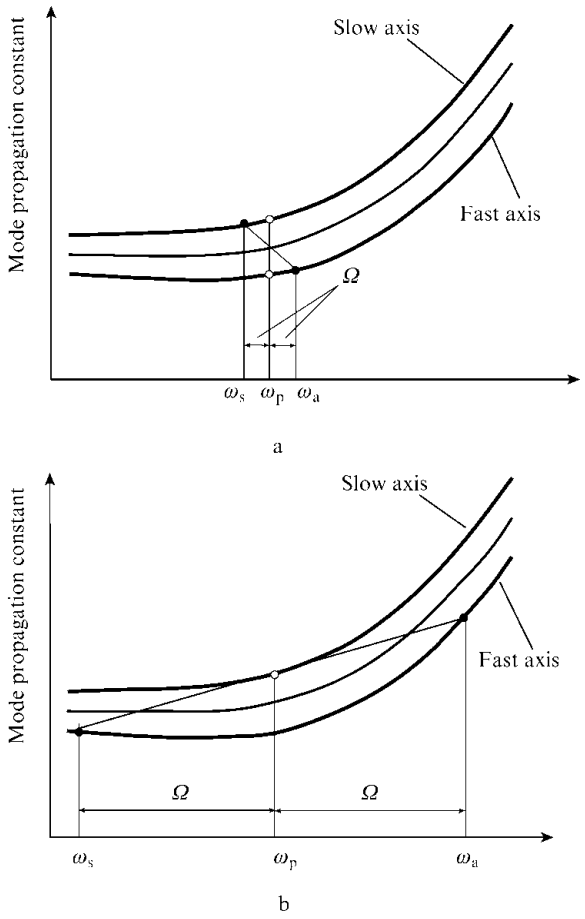

Figure 1. Schematic of phase matching in a polarisation-maintaining fibre.

The parametric gain coefficient depends on the total wave vector mismatch, Δk. In the case of nondegenerate pumping, it has the form [29]

$$g = [(\gamma P_0 r)^2 - (\Delta k/2)^2]^{1/2}.$$

Here $r = 2\sqrt{P_1 P_2}/P_0$ and $P_0 = P_1 + P_2$. In this study, the unpolarised pump power is equally divided between the slow and fast axes of the fibre, i.e. $P_1 = P_2 = \frac{1}{2}P_p$, where P_p is the pump power at the input of the birefringent fibre. Then we have $\Delta k_{NL} = \gamma P_p$ and $g = [(\gamma P_p)^2 - (\Delta k/2)^2]^{1/2}$.

For a parametric process to show up at relatively low cw pump powers, a seed signal wave is launched into the fibre. In the 'inexhaustible' pump source approximation ($P_p \gg P_s$), the idler power, P_i, depends in general on the signal power at the input of the fibre, $P_s(0)$; the pump power, P_p; nonlinearity coefficient, γ; fibre length, L; and gain coefficient, g (see e.g. Ref. [29]):

$$P_i(L) = P_s(0)\left(\frac{\gamma P_p}{g}\right)^2 \sinh^2(gL). \quad (1)$$

The single-pass unsaturated gain coefficient of the idler is given by

$$G = \frac{P_i(L)}{P_s(0)} = \left(\frac{\gamma P_p}{g}\right)^2 \sinh^2(gL). \quad (2)$$

At large wave vector mismatches ($\Delta k \gg \gamma P_p$), we have

$$G = (\gamma P_p L)^2 \frac{\sin^2(\Delta k L/2)}{(\Delta k L/2)^2}. \quad (3)$$

In this case, G well describes the wings of the idler gain profile. The nonlinearity of a fibre of length L can be quantified by $\xi = \gamma P_p L$. At a weak fibre nonlinearity ($\xi \leqslant 0.5$), the uncertainty in the gain calculated by (3) at the centre of the profile is within 10 %. In the case of exact phase matching ($\Delta k = 0$), relation (2) simplifies and the gain can be represented in the form $G_0 = \xi^2$. Therefore, the idler power is a linear function of signal power and a quadratic function of pump power:

$$P_i(L) = P_s(0)G_0 = P_s(0)(\gamma P_p L)^2 = P_s(0)\xi^2. \quad (4)$$

At low optical powers and a pump wavelength near 1 μm, the nonlinear contribution is far less than the contribution of the material dispersion, $\Delta k_{NL} \ll \Delta k_M$, and can be neglected. The type I phase matching condition, for a pump beam propagating along two axes of a polarisation-maintaining fibre (see e.g. Ref. [16]), then has the form

$$\Delta k = \Delta k_L = \beta_2 \Omega^2 - \delta n \Omega c^{-1} = 0, \quad (5)$$

where $\delta n = n_s - n_f$ is the difference between the refractive indices along the slow and fast axes (birefringence) of the fibre. Assuming that birefringence is a weak function of frequency, we obtain from (5) $\Omega = \delta n/(\beta_2 c)$. The birefringence of the Nufern PM980-XP fibre ($\delta n = 3.6 \times 10^{-4}$) is specified in its data sheet. The dispersion curve presented by the manufacturer is well fitted by the well-known relation $D(\lambda) = (S_0/4)(\lambda - \lambda_0^4/\lambda^3)$ [30], with $\lambda_0 = 1385.15$ and $S_0 = 0.08137$. The group velocity dispersion coefficient, β_2, was evaluated from the dispersion curve, $D(\lambda)$, and was found to be about 21 ps^2 km^{-1} at the pump wavelength used, $\lambda_p = 1048$ nm. Consequently, the frequency shift can be estimated at $\Omega/2\pi \approx 9.1$ THz, which is comparable to that reported by other groups [13, 14].

At a weak fibre nonlinearity ($\xi \ll 1$), the parametric gain bandwidth, $\Delta\Omega$, can be found using Eqn (3). It corresponds to the wave vector mismatch at which $\sin^2(\Delta k L/2) = 1$, i.e. $\Delta k L = \pm\pi$. The gain is then lower by a factor of $\pi^2/4$, and the wave vector mismatch is $\Delta k_s = 2\pi/L$. Differentiating Eqn (5) and substituting the frequency shift $\Omega = \delta n/(\beta_2 c)$, we can find the phase matching bandwidth, $\Delta\Omega$, from the wave vector mismatch:

$$\Delta k_s = \frac{\partial \Delta k}{\partial \Omega}\Delta\Omega = \left(2\beta_2\Omega - \frac{\delta n}{c}\right)\Delta\Omega = \frac{\delta n}{c}\Delta\Omega. \quad (6)$$

Consequently, the gain bandwidth is inversely proportional to the length and birefringence of the fibre: $\Delta\Omega = 2\pi c/(\delta n L)$. Near 1017 nm, the $\Delta\Omega$ of the idler wave in the PM980-XP fibre is 0.07 nm for a 35-m length and drops to 0.03 nm for a 85-m length. Thus, narrow-band pump and signal lasers should be used for efficient parametric oscillation in long fibres.

The above simplifications are valid at a weak nonlinearity ($\xi \ll 1$). Let us estimate the ξ of a 85-m length of the PM980-XP fibre. The fibre nonlinearity coefficient is $\gamma = 2\pi n_2/(\lambda_p A_{eff})$, where $n_2 \approx 2.3 \times 10^{-20}$ m^2 W^{-1} is the nonlinear refractive index [31] and A_{eff} is the effective mode area. Single-mode fibres are commonly thought to have a Gaussian mode field distribution and $A_{eff} = \pi(D/2)^2$, where D is the mode field diameter. The fibre under consideration has $D \approx (6.9 \pm 1)$ μm at 1060 nm. For $\lambda_p = 1048$ nm, we obtain a nonlinearity coefficient $\gamma \approx 3.7$ km W^{-1}. In birefringent fibres, however, the real part of third-order nonlinear susceptibility, $\chi^{(3)}$, is smaller for orthogonal polarisations in comparison with parallel polarisations [32]. For this reason, n_2 decreases by a factor of 3 and, accordingly, $\gamma \approx 1.23$ km^{-1} W^{-1}. Therefore, at a pump power of 4 W, nonlinearity is $\xi \approx 0.42$. The function $\sinh^2(x)$ in (2) can then be approximated by x^2 with a 6 % accuracy, and the idler power in the case of exact phase matching can be evaluated by Eqn (4).

3. Experimental and results

The experimental setup used is shown schematically in Fig. 2. A cw unpolarised pump beam and a signal beam were launched into a polarisation-maintaining fibre (Nufern PM980-XP) through a 30 : 70 fibre coupler. In our experiments, we used 35- and 85-m lengths of the fibre. The output beam was directed to the input of an optical spectrum analyser (OSA), which enabled observation of individual spectral lines. The pump source was a narrow-band cw ytterbium fibre laser with an emission wavelength $\lambda_p = 1048$ nm, emission linewidth under 0.1 nm and output power of up to 4 W. The signal source was another narrow-band cw ytterbium fibre laser, with a ring cavity and a tunable fibre Bragg grating (FBG) with axial compression in a ferrule, described elsewhere [33]. By compressing the FBG, we were able to vary the signal laser wavelength from 1093 to 1072 nm, thereby controlling the wave vector mismatch and adjusting the wavelength so as to meet the phase matching condition.

In our experiments, the signal wave corresponded to the Stokes component of FWM, and the idler wave, to the anti-Stokes component. At a signal wavelength $\lambda_s \approx 1080.3$ nm, the output spectrum contained an additional, so-called idler wave at $\lambda_i \approx 1017.7$ nm (Fig. 2, inset). Thus, the experimentally determined frequency shift between the idler and pump waves was $\Omega = 8.6$ THz, which is comparable to the above estimate.

Using the OSA, we obtained the parametric oscillation spectrum. Figure 3 shows idler spectra for the signal wavelength, λ_s, tuned around the phase matching wavelength of a 85-m length of the PM980-XP fibre. The pump and signal powers, P_p and P_s, were 2.8 and 1.7 W, respectively. The pump linewidth, $\Delta\lambda_p$, was within 0.05 nm, and the signal linewidth, $\Delta\lambda_s$, was 0.11 nm.

As seen in Fig. 3, increasing the phase mismatch distorts the shape of the spectra, producing additional dips, which correspond to the minima of the function $\mathrm{sinc}^2(x)$. Unfortu-

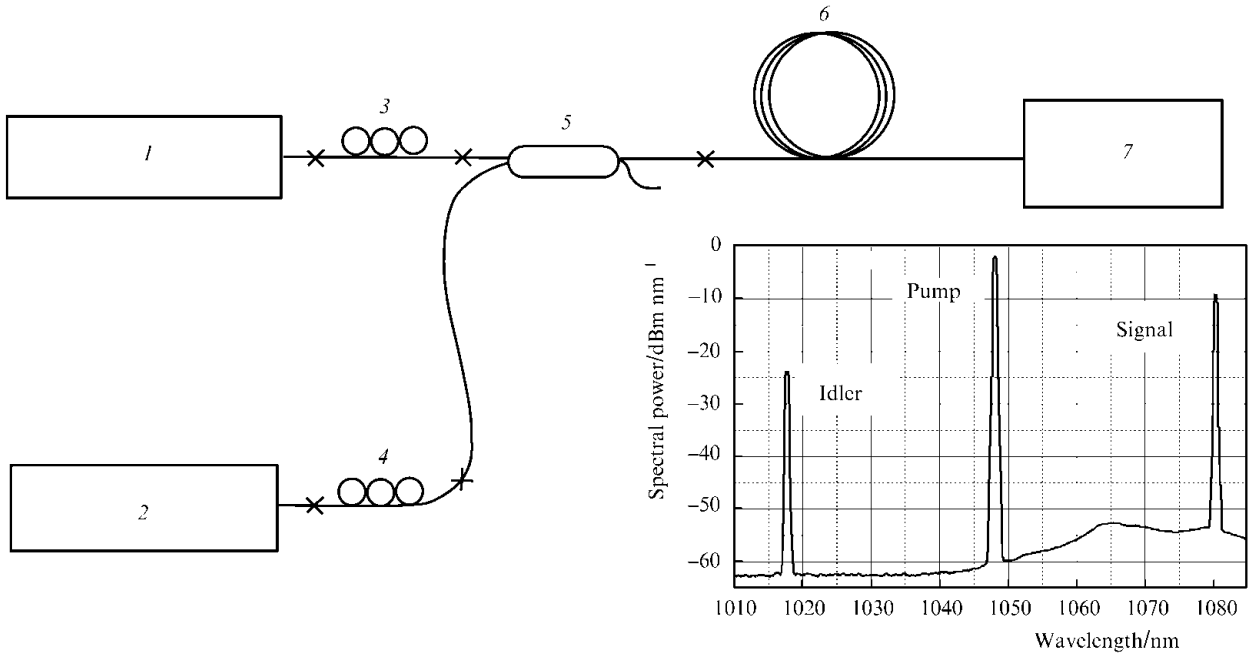

Figure 2. Schematic of a single-pass cw parametric converter: (*1*) pump laser; (*2*) tunable signal laser; (*3, 4*) polarisation controllers; (*5*) 30 : 70 fibre coupler; (*6*) Nufern PM980-XP polarisation-maintaining fibre; (*7*) optical spectrum analyser.

nately, the instrumental function of the OSA at the best resolution was 0.025 nm, which exceeded the period of $\mathrm{sinc}^2(x)$. For this reason, the minima were broadened and poorly discernible on the spectrum analyser. The dots in the figure represent the theoretical parametric gain profile calculated using relations (2) and (6) with fibre parameters $\gamma = 1.23\ \mathrm{km^{-1}\ W^{-1}}$, $\delta n = 3.6 \times 10^{-4}$, and $L = 85$ m, at $P_\mathrm{p} = 2.8$ W.

The power of the waves involved in the FWM process was determined as follows: First, the relative output power distribution was measured using the spectrum analyser and emission lines. Next, the OSA was replaced by a power meter and the output power was determined. The measured output power was used to calibrate the idler, signal, and pump powers.

Figure 4 shows the measured idler power (data points) as a function of pump power. The data show parabolic behaviour, in agreement with theory. The $P_\mathrm{i}(P_\mathrm{p})$ curve (solid line) was calculated using the measured P_p and P_s and the relation

$$P_\mathrm{i}(L) = \eta P_\mathrm{s} P_\mathrm{p}^2, \tag{7}$$

where η is proportional to FWM efficiency. Comparison of Eqns (4) and (7) shows that η is a quadratic function of the fibre length and nonlinearity coefficient: $\eta = \frac{1}{2}(\gamma L)^2$. The factor $\frac{1}{2}$ results from the fact that the FWM process involves only that part of the signal wave which is polarised along the slow axis, so the effective signal power decreases by a factor of 2. We fitted the experimental data by varying η. From the data in Fig. 4, we obtained $\eta = 6 \times 10^{-3}\ \mathrm{W^{-2}}$.

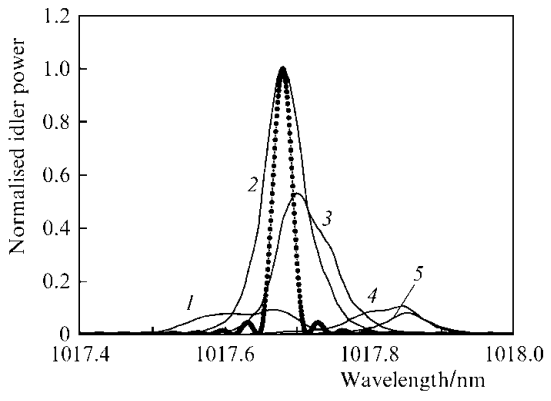

Figure 3. Idler wavelength tuning at a fibre length $L = 85$ m: $\lambda_\mathrm{s} =$ (*1*) 1080.46, (*2*) 1080.37, (*3*) 1080.31, (*4*) 1080.19 and (*5*) 1080.14 nm. The dots represent the parametric gain profile.

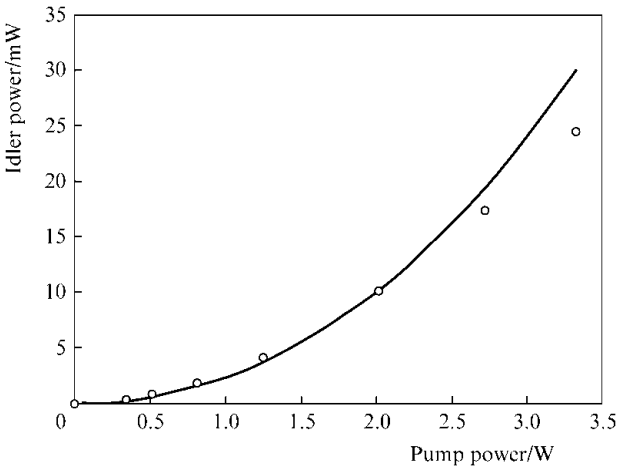

Figure 4. Measured (data points) and calculated (solid line) idler power as a function of pump power at $L = 85$ m and $P_\mathrm{s} \approx 0.8$ W.

Figure 5 shows the idler power as a function of signal power for fibre lengths of 35 and 85 m. The plots are seen to be linear at low signal powers, in agreement with theory, but with increasing signal power their slope decreases. For clarity, the P_i values at a pump power of 0.56 W are increased by a factor of 10.

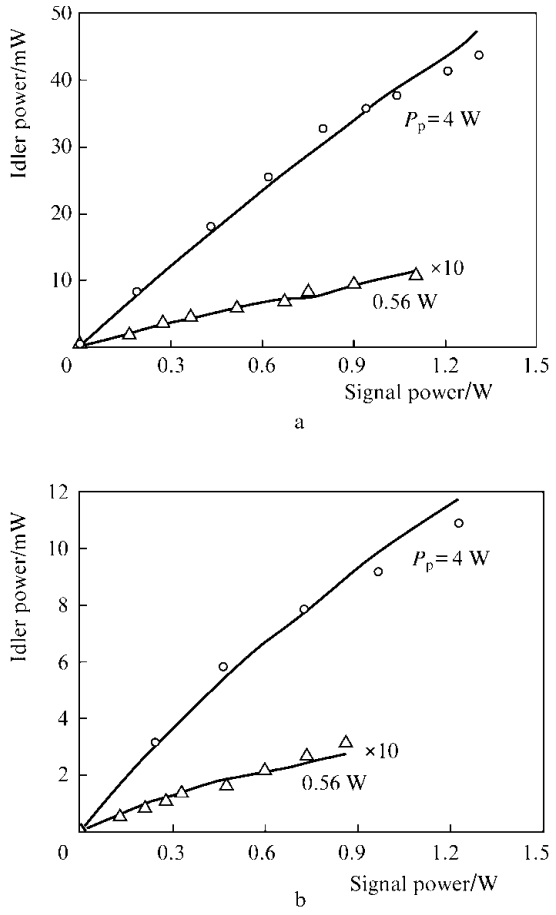

Figure 5. Measured (data points) and calculated (solid lines) idler power as a function of signal power at $L = 85$ (a) and (b) 35 m.

The curves were obtained by substituting the measured P_p and P_s into Eqn (4) and adjusting η so as to achieve the best fit to the experimental data. The calculated curves have small breaks, which are attributable to the fact that, with increasing signal power, P_s, the pump power, P_p, decreased by about 20 %. At an input P_p of 4 W and $L = 85$ m, the power of the generated wave exceeded 40 mW.

The present results are summarised in Table 1, which lists the fitting coefficients η and the calculated fibre nonlinearity coefficients $\gamma = \sqrt{2\eta}/L$.

Table 1. Coefficients η and the corresponding calculated fibre nonlinearity coefficients γ.

L/m	P_p/W	$\eta/10^{-3}$ W^{-2}	γ/km^{-1} W^{-1}
85	4	5	0.83
	0.56	7.2	1.00
35	3.8	1.6	1.14
	0.5	3	1.56

4. Discussion

It follows from Fig. 3 that the theoretical parametric gain profile is half as wide as the idler line. The key factor is the width of the instrumental function of the spectrum analyser, which is comparable to the gain bandwidth. In the calculations above, we assumed that the pump and signal lines had zero width, but in practice the emission lines of lasers have a finite width. As a result, the phase matching condition is met for a variety of longitudinal modes of the two lasers, leading to broadening of the idler spectrum. It is also worth noting that changing the signal wavelength by 0.23 nm shifts the idler peak by 0.18 nm, indicating that the wings of the idler spectrum begin to contribute to the FWM process. Nevertheless, the observed gain band is rather narrow, and even a change in λ_s by just 0.06 nm reduces the idler power by a factor of 2.

It might be expected that the power of the generated wave can be increased further by raising the pump and signal powers. It is however seen from Figs 3 and 4 that, as these powers are raised, the experimental data deviate from the calculated curve, with idler power saturation. The saturation is particularly significant at high P_p. Moreover, it follows from Table 1 that, at a given fibre length, the coefficient η increases with decreasing pump power, which means that the efficiency of the parametric process decreases with increasing input powers.

The origin of the idler power saturation can be understood by examining how the width of the emission spectra of the lasers responds to an increase in emission power and, accordingly, in the magnitude of nonlinear effects. FWM of various longitudinal cavity modes leads to broadening of the output spectrum, like in the case of Raman lasers [34]. The pump linewidth is $\Delta\lambda_p = 0.03$ nm at $P_p = 0.5$ W and 0.07 nm at $P_p = 4$ W. Figure 6 shows the measured broadening of the signal laser line, $\Delta\lambda_s$, as a function of signal power, P_s. It can be seen that, even at $P_s = 0.3$ W, $\Delta\lambda_s$ exceeds the parametric gain bandwidth for a 85-m-long fibre (calculated bandwidth, 0.03 nm). At a signal power of 1 W, it exceeds the gain bandwidth for a 35-m-long fibre (0.07 nm). Consequently, the broadening of the emission spectra of the lasers with increasing power markedly reduces the FWM efficiency.

Since $\Delta\Omega$ at low P_p values is less than or comparable to

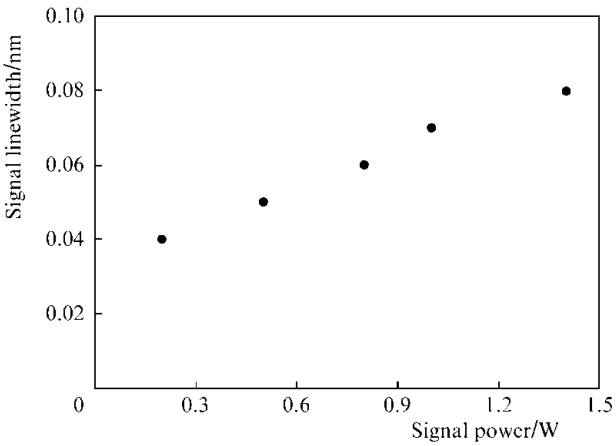

Figure 6. Measured broadening of the signal laser line as a function of output power.

the laser linewidths, it is reasonable to expect that, in this case, broadening of the pump and signal spectra has little effect on the idler power. The nonlinearity coefficient, γ, of the Nufern PM980-XP fibre can then be estimated from experimental data as the average of 1.56 and 1 km^{-1} W^{-1} (Table 1): $\gamma \approx 1.3$ km^{-1} W^{-1}. The γ for orthogonal polarisations is a factor of 3 smaller than that for parallel polarisations, so actually $\gamma = 3.9$ km^{-1} W^{-1} for this type of fibre, which agrees with the calculated γ, 3.7 km^{-1} W^{-1}, within 6 %.

According to (4), the single-pass conversion efficiency of the cw parametric process, $P_i(L)/P_s(0)$, in the $\xi \ll 1$ approximation is ξ^2. In our experiment at $L = 85$ m, $\gamma = 1.3$ km^{-1} W^{-1} and $P_p = 4$ W, nonlinearity was $\xi = 0.44$, which is comparable to nonlinearities in experiments concerned with cw parametric up-conversion in photonic crystal fibres [12, 27]. Despite the large nonlinearity coefficient in such fibres, their ξ does not exceed 0.6 [12] or 0.38 [27] because of the low pump power ($P_p \leqslant 0.2$ W). As a result, the power of the generated wave in those studies was under 1 mW, and the experimentally determined conversion efficiency was within 0.3 %. In this study, at $\xi = 0.44$ the experimentally determined conversion efficiency was 3.3 %. The high conversion efficiency may be due to the fact that we used a more homogeneous fibre and narrower band light sources in comparison with previous studies [12, 27].

It is also worth pointing out that the use of single-frequency lasers or high-power ytterbium sources with an emission linewidth less than the parametric gain bandwidth can raise the conversion efficiency from 3.3 % to the theoretically possible 20 % at the same pump and signal powers. Moreover, a decrease in pump and signal wavelengths will enable one to produce a light source tunable in the range 1000 – 1025 nm, that is, outside the emission line of conventional ytterbium fibre lasers.

Parametric processes in polarisation-maintaining fibres may have large frequency shifts (Fig. 1b). For efficient parametric oscillation, input light should then be polarised in a certain manner.

5. Conclusions

Previous studies concerned with cw parametric up-conversion at wavelengths $\lambda \leqslant 1$ μm employed photonic crystal fibres. In such fibres, phase matching was ensured near the zero-dispersion wavelength of the fibre and the conversion efficiency did not exceed 0.3 %. In this study, using polarisation phase matching we have demonstrated for the first time cw parametric oscillation in a birefringent fibre, with an increase in frequency by 8.6 THz. At a pump power of 4 W and fibre length of 85 m, the conversion efficiency was 3.3 %.

Efficiency measurements at low pump powers have led us to conclude that, by narrowing the emission spectra of the lasers to the parametric gain bandwidth, the conversion efficiency can be raised from 3.3 % to 20 %. Note, however, that a serious obstacle in this context may be fluctuations of fibre parameters, which would cause dispersion variations along the length of the fibre.

It is also worth pointing out that, using tunable pump and signal sources, one can obtain a narrow-band polarised light source operating in the range 1000 – 1025 nm, that is, outside the emission line of standard ytterbium fibre lasers.

Acknowledgements. This work was supported by the RF Ministry of Education and Science and the Siberian Branch of the Russian Academy of Sciences (integrated research project).

References

1. Chen A.Y.H., Wong G.K.L., Murdoch S.G., Leonhardt R., Harvey J.D., Knight J.C., Wadsworth W.J., Russell P.St.J. *Opt. Lett.*, **30**, 762 (2005).
2. Tombelaine V., Labruyere A., Kobelke J., Schuster K., Reichel V., Leproux P., Couderc V., Jamier R., Bartelt H. *Opt. Express*, **17**, 15392 (2009).
3. Stolen R.H., Leibolt W.N. *Appl. Opt.*, **15**, 239 (1976).
4. Angelow A.K., Kircheva P.P. *Appl. Opt.*, **33**, 3203 (1994).
5. Sharping J.E. *J. Lightwave Technol.*, **26** (14), 2184 (2008).
6. Marhic M.E., Wong K.K.Y., Kazovsky L.G., Tsai T.E. *Opt. Lett.*, **27**, 1439 (2002).
7. Solodyankin M.A., Medvedkov O.I., Dianov E.M. *Proc. Conf. ECOC'05* (Glasgow, UK, 2005) Vol. 1, pp 47, 48.
8. Wong K.L., Murdoch S.G., Leonhardt R., Harvey J.D., Marie V. *Opt. Express*, **15**, 2947 (2007).
9. Gershikov A., Shumakher E., Willinger A., Eisenstein G. *Opt. Lett.*, **35**, 3198 (2010).
10. Malik R., Marhic M.E. *Proc. Nat. Fiber Opt. Eng. Conf., OSA Techn. Dig.* (San Diego, OSA, 2010) paper JWA18.
11. Deng Y., Lin Q., Lu F., Agrawal G.P., Knox W.H. *Opt. Lett.*, **30**, 1234 (2005).
12. Yatsenko Yu.P., Levchenko A.E., Pryamikov A.D., Kosolapov A.F., Semenov S.L., Dianov E.M. *Kvantovaya Elektron.*, **35**, 715 (2005) [*Quantum Electron.*, **35**, 715 (2005)].
13. Park H.G., Park J.D., Lee S.S. *Appl. Opt.*, **26**, 2974 (1987).
14. Chee J.K., Liu J.M. *Opt. Lett.*, **14**, 820 (1989).
15. Xiong C., Wadsworth W.J. *Opt. Express*, **16**, 2438 (2008).
16. Jain R.K., Stenersen K. *Appl. Phys. B*, **35**, 49 (1984).
17. Lantz E., Gindre D., Maillotte H., Monneret J. *J. Opt. Soc. Am. B*, **14**, 116 (1997).
18. Yang T., Gao P. *Opt. Lett.*, **15**, 1002 (1990).
19. Murdoch S.G., Leonhardt R., Harvey J.D. *J. Opt. Soc. Am. B*, **14**, 3403 (1997).
20. Chiang K.S., Lor K.P., Chow Y.T. *Opt. Lett.*, **22**, 510 (1997).
21. Stolen R.H., Bosch M.A., Lin Ch. *Opt. Lett.*, **6**, 213 (1981).
22. Ohashi M., Kitayama K., Shibata N., Seikai S. *Opt. Lett.*, **10**, 77 (1985).
23. Kitayama K., Ohashi M. *Appl. Phys. Lett.*, **41**, 619 (1982).
24. Shibata N., Ohashi M., Kitayama K., Seikai S. *Opt. Lett.*, **10**, 154 (1985).
25. Kitayama K., Seikai S., Uchida N. *Appl. Phys. Lett.*, **41**, 322 (1982).
26. Kruhlak R.J., Wong G.K., Chen J.S., Murdoch S.G., Leonhardt R., Harvey J.D., Joly N.Y., Knight J.C. *Opt. Lett.*, **31**, 1379 (2006).
27. Andersen T.V., Hilligsoe K.M., Nielsen C.K., Thogersen J., Hansen K.P., Keiding S.R., Larsen J.J. *Opt. Express*, **12**, 4113 (2004).
28. Jiang R., Saperstein R.E., Alic N., Nezhad M., McKinstrie C.J., Ford J.E., Fainman Y., Radic S. *J. Lightwave Technol.*, **25**, 58 (2007).
29. Agrawal G.P. *Nonlinear Fiber Optics* (San Diego: Acad. Press, 2001).
30. Keiser G. *Optical Fiber Communications* (Singapore: McGraw-Hill, 1991).

31. Namihira Y., Miyagi K., Kaneshima K., Tadakuma M., Vinegoni C., Pietra G., Kawanami K. *Techn. Dig. 12th Symp. on Opt. Fiber Measur.* (Boulder, 2002) pp 15–18.
32. Schulz R., Harde H. *J. Opt. Soc. Am. B*, **12**, 1279 (1995).
33. Babin S.A., Kablukov S.I., Vlasov A.A. *Laser Phys.*, **17**, 1323 (2007).
34. Babin S.A., V. Churkin D.V., Ismagulov A.E., Kablukov S.I., Podivilov E.V. *J. Opt. Soc. Am. B*, **24**, 1729 (2007).